Research Square

Preprints are preliminary reports that have not undergone peer review.
They should not be considered conclusive, used to inform clinical practice,
or referenced by the media as validated information.

Oxytocin neurons in the paraventricular nucleus of the hypothalamus circuit-dependently regulates social behavior, which malfunctions in BTBR mouse model of autism

Hiroyuki Arakawa (harakawa@med.u-ryukyu.ac.jp)
University of Ryukyus https://orcid.org/0000-0002-6175-9278
Yuki Higuchi
University of the Ryukyus
Akihiko Ozawa
Florida Atlantic University

Article

Keywords:

Posted Date: March 1st, 2023

DOI: https://doi.org/10.21203/rs.3.rs-2621359/v1

License: This work is licensed under a Creative Commons Attribution 4.0 International License.
Read Full License

Abstract

Oxytocin (OXT) a neuropeptide synthesized in the hypothalamic nuclei has a variety of function including socio-emotional processes in mammals. While the neural circuits and signaling pathways in central OXT converge in the paraventricular nucleus of the hypothalamus (PVN), we illuminate specific function of discrete PVN OXT circuits, which connect to the medial amygdala (MeA) and the bed nucleus of the stria terminalis (BnST) in mouse models. The $OXT^{PVN}\rightarrow^{BnST}$ projections are innervated from entire portions of the PVN, while those $OXT^{PVN}\rightarrow^{MeA}$ projections are asymmetrically innervated from the posterior portion of the PVN. Compared with OXT neurons in B6 wild type mice, BTBR mice that are recognized as a behavior-based autism model exhibited defect in the $OXT^{PVN}\rightarrow^{BnST}$ projection. We demonstrate that chemogenetic activation of $OXT^{PVN}\rightarrow^{MeA}$ circuit enhances anxiety-like behavior and facilitates social approach behavior, while activation of $OXT^{PVN}\rightarrow^{BnST}$ circuit suppresses anxiety-like behavior along with inhibiting social approach. This chemogenetic manipulation on the $OXT^{PVN}\rightarrow^{BnST}$ circuit proves ineffective in BTBR mice. Accordingly, chemogenetic activation of OXT^{PVN} neurons that stimulate both OXT circuits induces OXT receptor expressions in both MeA and BnST as with those by social encounter in B6 mice. The induction of OXT receptor genes in the BnST was not observed in BTBR mice. These data support the hypothesis that OXT circuits serve as a regulator for OXT signaling in PVN to control socio-emotional approach/avoidance behavior, and a defect of $OXT^{PVN}\rightarrow^{BnST}$ circuit contributes to autism-like social phenotypes in BTBR mice.

Introduction

Social interaction is a fundamental behavior in all animal species for sustaining adaptive life and well-being. Engaging in positive social (i.e., prosocial) interactions robustly benefits health across the lifespan [1–3]. The disruption of prosocial relationships has emerged as a major symptom in many psychiatric diseases and neurodegenerative diseases [4–7]. Oxytocin (OXT) is a neuropeptide involved in a key mechanism that regulates prosocial behavior, as evidenced in several different species, including humans [8–10]. Central OXT synthesis occurs in the paraventricular nucleus (PVN) and the supraoptic nucleus (SON) of the hypothalamus and in the accessory magnocellular nuclei of the hypothalamus, such as strio- and septo-hypothalamic nuclei [10–11]. The central OXT is mainly transported via axonal projections from the PVN, distributed to various brain regions, including the basal ganglia area, such as nucleus accumbens, septal nucleus, bed nucleus of the stria terminalis (BnST), medial amygdala (MeA), and paraventricular thalamic nucleus, and mid brain areas including the raphe nucleus and periaqueductal gray [12–13]. In particular, the $OXT^{PVN}\rightarrow^{MeA}$ projections are required for the processing prosocial approach behavior [14–16], while those $OXT^{PVN}\rightarrow^{BnST}$ contribute to social avoidance by circuit-specific OXT action [17].

The PVN is a complex, multifunctional and multitransmitter nucleus, which modulate many CNS processes, including stress-related hormonal regulation [18]; thus, either social interaction or exploration of unfamiliar objects induces neural activation in the PVN [19]. Activation of the PVN neurons by these

stimulus exposures also follows OXT release and OXT-ergic circuit-specific processing, which would be determined by the type and intensity of stimuli exposed. Abnormalities in either the OXT peptide or its receptor have been associated with social deficits that are prevalent in many psychiatric and neurodevelopmental disorders, including autism spectrum disorders (ASD) [20–21]. While whole-brain (e.g., intranasal) treatment with OXT failed to affect prosocial behavior in mice [22] and alleviate ASD symptoms in clinical trials [23], circuit-specific processing of OXT via the complex PVN network underlies for appropriate expressions of prosocial behaviors.

Mice are a highly social species that provide an exceptional tool for elucidating the neural mechanisms underlying prosocial behavior and its deficits [24]. Multiple lines of evidence have indicated that BTBR T + Itpr3tf/J (BTBR) mouse serves as a behavior-based ASD model resembling the characteristics of human ASD, including impaired prosocial interaction and persistent, repetitive behaviors [25–26]. A decreased neural activation of the PVN in BTBR mice in response to the presence of social stimuli compared to that in control mouse strain (e.g., C57BL/6J; B6 mice) has been documented [27–29]. Altered OXT neuronal morphology in the PVN was also evident in both sexes of BTBR mice compared to B6 mice [27, 29]. We hypothesized that (1) OXT signaling in the PVN is relayed via circuit-specific processes to control appropriate expression of prosocial behavior, and that (2) mal-formation or disconnection of these OXT circuits underlies social deficits exhibited by BTBR mice. Using immunohistochemical mapping of neural activity patterns and cell-type specific tracing of OXT projections, we identify modified neural activity and altered OXT projecting patterns in the PVN of BTBR mice. Our data obtained by chemogenetic manipulation of PVN neurons demonstrate that two massive OXT projections, $OXT^{PVN \rightarrow MeA}$ and $OXT^{PVN \rightarrow BnST}$, discretely regulate social and non-social behaviors, and a modification of these projections and binding receptor expressions are determinants for social deficits in BTBR mice. In summary, the data demonstrate a circuitry role for PVN OXT signaling in the expression of prosocial behavior, and reveal a possible OXT mechanism underlying deficiency in BTBR mice as an ASD mouse model.

Materials And Methods

Animals

BTBR T + Itpr3tf/J (BTBR) mice (stock # 002282) and C57BL/6J (B6) mice (stock # 000664) of both sexes were originally purchased from The Jackson Laboratory (Bar Harbor, ME, USA), were used as subject and stimulus mice. They were bred and maintained in the colony room of a facility at the University of the Ryukyus Faculty of Medicine, Japan. The mice were housed in groups of three or four in standard shoebox cages (28 × 22.5 × 14 cm height) with water and food provided ad libitum. The vivarium was maintained at 50% humidity and 23 ± 1˚C, with a 12-h light/dark cycle (lights on at 08:00). All procedures including animal care and use were performed in line with the National Institutes of Health Guide for the Care and Use of Laboratory Animals that comply with the ARRIVE guidelines and approved

by the Institutional Laboratory Animal Care and Use Committee at the University of the Ryukyus Graduate School of Medicine.

Experimental design

For full description of methods, see Supplementary information. Briefly, we firstly measured neural activity in the PVN sub-portions (rostral to caudal) and related brain regions of B6 (n = 22) and BTBR mice (n = 21) in response to a novel social or object encounter. Then we conducted a series of behavioral tests to assess social and non-social profiles relevant to autism-like behaviors in B6 and BTBR mice. Our test battery consisted of a set of anxiety/locomotor task (the elevated plus maze), social behavior task (the modified three-chamber test), and defensive behavior task (odor defense test). These subject mice including male and female received a bilateral AAV injection for DREADD manipulation and assigned into one of five AAV conditions (Vehicle; B6, n = 24, BTBR, n = 26, ns PVN; B6, n = 22, BTBR, n = 20, OXT-PVN; B6, n = 20, BTBR n = 20, OXT-MeA; B6, n = 19, BTBR, n = 17 and OXT-BnST; B6, n = 14, BTBR, n = 14). Testing was performed in tandem with small groups of mice consisting of three-to-four cohorts of animals at different times. Following a completion of behavioral testing, AAV transduction in the targeted brain sites was histologically verified by microscopy with transduced fluorescence and immunohistochemical staining of OXT neurons. Finally, mRNA expressions of targeted genes in social processing brain regions following a social encounter or chemogenetic activation of OXT^{PVN} neurons were evaluated in B6 (n = 32) and BTBR mice (n = 30).

Results

PVN neuronal activity in response to social and non-social encounter

We firstly confirmed neural responses of the PVN sub-regions to social and non-social stimuli in B6 and BTBR mice. To map neural activity patterns in the PVN following exposure to novel social and non-social (object) stimuli, we performed immunohistochemistry for c-Fos across the rostral-caudal divides of the PVN (Fig. 1A,C) and its projecting regions; MeA (Fig. 1F), BnST (Fig. 1D,E), and LS (Fig. 1G) in B6 and BTBR mice that were exposed to a social (a novel same-sex mouse) or non-animated object, or remained in a home cage as a no exposure control (Fig. 1H)(see **Fig. S1**). For B6 mice, across the rostral to caudal portions of the PVN, significantly more cells expressing c-Fos in response to either social or non-social stimuli compared to the control condition were documented (Fig. 1A,B,C). For BTBR mice, however, the induction of c-Fos was found through the middle to caudal portions of the PVN only by an object, but not social, exposure. This effect mapped c-Fos induction disappeared in the rostral portion of the PVN. In the projecting regions from the PVN, the numbers of c-Fos + cells were increased both by social and non-social (object) exposures in B6 mice, and these were blunted in BTBR mice. Accordingly, sniffing/contact investigation towards exposed stimuli was demonstrated in both B6 and BTBR mice; however, these were attenuated in BTBR mice when confronted with a social stimulus (Fig. 1I). Therefore, a blunted c-Fos

induction in targeted regions in response to social encounter exhibited by BTBR mice is covariant with decreased social investigation.

Oxytocinergic neural projection patterns reveal strain difference

OXT neurons of the PVN are primarily responsible for the innervation of forebrain regions [30]. While dendritic OXT release are also evident [31], OXT neurons of the PVN send axonal projections to various distances of brain regions, including the basal forebrain area, such as septal nucleus, BnST, and MeA, and several thalamic and hind brain regions [12–13]. We chose two massive OXT projecting regions, MeA and BnST, based on functional contribution to the regulation of social behavior [14, 16–17]. Immunohistchemical analysis confirmed that OXT neurons are distributed across the rostral to caudal portions of the PVN in both B6 and BTBR mice, while densities of OXT neurons are lower in BTBR mice than those in B6 mice constantly across the PVN sub-portions (Fig. 2C,D). Using a retrograde AAV vector encoding mCherry with selective OXT promoter (retroAAV-pOXT;hM3Dq-mCherry), we investigated the distribution of OXT neurons projecting to the BnST or MeA within the PVN neuronal population. $OXT^{PVN \rightarrow BnST}$ neurons are distributed widely across the rostral to caudal portions of the PVN in B6 mice, while these $OXT^{PVN \rightarrow BnST}$ neurons are present in only trace amounts in BTBR mice (Fig. 2G). Furthermore, there was no strain difference in the ratio of $OXT^{PVN \rightarrow MeA}$ neurons between B6 and BTBR mice (Fig. 2H). The $OXT^{PVN \rightarrow MeA}$ neurons tend to locate massively in the caudal portion of the PVN in both B6 and BTBR mice.

The $OXT^{PVN \rightarrow MeA}$ circuits facilitate anxiety-like behavior differs from the $OXT^{PVN \rightarrow BnST}$ circuits

The EPM is a popular test method to measure anxiety along with locomotor activity in rodent models [32]. BTBR mice display a variable profile of anxiety-like behaviors in the EPM (e.g., increase or decrease) when compared with B6 strains [25, 33–34, 62]. In present study, both male and female BTBR mice exhibited a low anxious profile in the EPM, with an increased locomotor activity and enhanced open arm time compared with control B6 mice (**Fig. S3**). Otherwise, sex differences of the behavioral performance in BTBR strain as well as B6 strain were not consistent in this test.

The PVN is a center brain region for stress response [35] and anxiety behavior [36]. While OXT is known to play a modulatory role in anxiety behavior, the effects of exogeneous OXT are still variable [37] and the brain regions that transmit OXT information from the PVN for proper execution of anxiety behavior have not been identified. We applied chemogenetic manipulation on the PVN neurons to determine the cell-type and projection-specific function of the PVN circuits. In particular, we bilaterally injected AAV vector with low transduce tropism via ubiquitin promoter (AAV8-EF1a:hM3Dq; Ns PVN, labeling global PVN neurons) or OXT specific promoter (AAV8-pOXT:hM3Dq; OXT-PVN) into the PVN (Fig. 3A and **Fig. S2**). We also injected AAV vectors with retrograde tropism via OXT promoter (retro-AAV-pOXT:hM3Dq) at the MeA (OXT-

MeA) and the BnST (OXT-BnST) solely, to manipulate $OXT^{PVN}\rightarrow^{MeA}$ and $OXT^{PVN}\rightarrow^{BnST}$ projections, respectively. In this scenario, cell expressing hM3(Dw) are categorized as various cell types in the PVN region (Ns PVN); specifically OXT neurons in the PVN (OXT-PVN); $OXT^{PVN}\rightarrow^{MeA}$ projection neurons (OXT-MeA); or $OXT^{PVN}\rightarrow^{BnST}$ projection neurons (OXT-BnST). This manipulation induced selective excitation of targeted neurons by an injection of a DREADD ligand, Compound 21 (C21). In the EPM, open arm time was decreased by activating $OXT^{PVN}\rightarrow^{MeA}$ (OXT-MeA) but was increased when the $OXT^{PVN}\rightarrow^{BnST}$ projection (OXT-BnST) was activated in B6 mice (Fig. 3D). For BTBR strain, the open arm time was decreased by activating global PVN neurons (Ns PVN) or $OXT^{PVN}\rightarrow^{MeA}$ projection (OXT-MeA) (Fig. 3E). There was no impact observed on locomotor activity in both mouse strains under the current DREADD manipulation conditions (Fig. 3B,C). These data suggest that activation of $OXT^{PVN}\rightarrow^{MeA}$ neurons is consistently anxiogenic in both B6 and BTBR mice, while $OXT^{PVN}\rightarrow^{BnST}$ neurons is anxiolytic in B6 mice but no effect in BTBR mice.

OXT circuits determine controlling prosocial behavior

The OXT neurons play a critical role in processing social approach and avoidance in a variety of contexts, which implies circuit-specific OXT action. The $OXT^{PVN}\rightarrow^{MeA}$ neurons are responsive to facilitate social approach to conspecifics [15–16], while the $OXT^{PVN}\rightarrow^{BnST}$ neurons promote social avoidance in female California mice [38] and reduce social approach in stressed mice [17]. We provide evidence that circuit-specific control of OXT in prosocial behavior is also strain-dependent.

As consonantly shown in various literatures, both male and female BTBR mice demonstrate behavioral traits relevant to autism, including reduced social approach towards familiar (c.f., same strain) or unfamiliar (c.f., different strain) social stimuli, compared to B6 controls (**Fig. S3**). Using chemogenetic manipulation, we uncovered cell-type and circuit-dependent regulation of these social behavioral traits in B6 and BTBR mice. When confronted with a same-sex familiar opponent (i.e., B6 stimulus mouse), activation of OXT^{PVN} neurons (OXT-PVN), but not those of global PVN neurons (ns PVN), decreased social approach of B6 mice (Fig. 3H). An activation of specific $OXT^{PVN}\rightarrow^{BnST}$ neurons (OXT-BnST) but not $OXT^{PVN}\rightarrow^{MeA}$ neurons (OXT-MeA) reduced social approach in B6 mice (Fig. 3H). However, these chemogenetic activations of PVN neurons had little impact on social approach to familiar (i.e., BTBR stimulus mouse) opponents in BTBR mice (Fig. 3I). These behavioral profiles in response to chemogenetic activation of PVN neurons differ dependent on familiarity of the opponents. When confronted with a same-sex unfamiliar mouse, activations of global PVN neurons (ns PVN), OXT^{PVN} neurons (OXT-PVN), and $OXT^{PVN}\rightarrow^{BnST}$ neurons (OXT-BnST) decreased social approach in B6 mice (Fig. 3J). The social approach of BTBR mice toward an unfamiliar mouse was enhanced by activation of global PVN neurons (ns PVN), OXT^{PVN} neurons (OXT- PVN), and $OXT^{PVN}\rightarrow^{MeA}$ neurons (OXT-MeA), but not by those $OXT^{PVN}\rightarrow^{BnST}$ neurons (OXT-BnST)(Fig. 3K). While activation of global PVN neurons or OXT neurons in the PVN produced undirected effects on social approach in B6 and BTBR mice, selective activation of $OXT^{PVN}\rightarrow^{MeA}$ neurons sufficiently maintained (or enhanced) substantial level of social

approach in both B6 and BTBR mice, and those of $OXT^{PVN}\rightarrow^{BnST}$ neurons reduced social approach in B6 mice but maintained lower levels in BTBR mice.

Distinct PVN circuits regulate non-social behavioral profile relevant to autism-like traits

BTBR mouse model has been associated with deficits in social communication and a pronounced engagement in repetitive behavior [25, 39]. Excessive self-grooming and persistent digging and burying the floor bedding materials (e.g., sawdust or corncob) or novel obstacles (e.g., embedded marbles) are considered to represent these later pathological states [40, 41]. The characteristics of BTBR mice suggest that variant circuitry controlling exploratory and defensive behaviors underlying their atypical behaviors needs to be elucidated. We conducted an olfactory defense test, in which mice display defensive behaviors towards exposures of neutral (ie. banana odor) and predatory (ie., fox urine compound) odor cues [42]. B6 mice displayed flexible sniff-immobile defensive patterns in tune with the type of odor stimuli, by decreased sniffing and increased immobile toward predatory aversive odor compared to those toward neutral odor (**Fig. S3E**). While BTBR mice exhibited reduced susceptibility of sniff/immobile response, they showed attenuated immobile time compared to B6 mice (**Fig. S3F**). In addition, BTBR mice exhibited a heightened levels of digging the bedding material and self-grooming compared to B6 mice (**Fig. S3G,H**).

To rule out the PVN circuitry function in these defensive components, we assessed the impact of chemogenetic manipulation on these behaviors. B6 mice altered their sniff-immobile profile following an activation of $OXT^{PVN}\rightarrow^{BnST}$ neurons (i.e., PVN-BnST) when confronted with a neutral natural odor (Fig. 4A,C), and following an activation of the global PVN neurons (i.e., ns PVN) when confronted with predatory odor (Fig. 4E,G). In contrast, BTBR mice did not show any change in sniff-immobile strategy towards odor stimuli via either chemogenetic PVN activations (Fig. 4F,H). Furthermore, an activation of the global PVN neurons (i.e., ns PVN) stimulated increased digging and self-grooming behavior in B6 mice (Fig. 4I,K) and self-grooming in BTBR mice (Fig. 4J,L). These data indicate that the activation of $OXT^{PVN}\rightarrow^{BnST}$ neurons induces enhanced exploratory, but not defensive properties in B6 mice and this circuitry may not be responsive in BTBR mice. Global, but non OXT, PVN activation produces modification of other defensive behaviors, including immobile defense and digging and grooming behaviors, suggesting that these behavioral components are regulated by non OXT^{PVN} neurons.

mRNA expression profiles following chemogenetic OXT^{PVN} activation and social encounter

To validate OXT circuitry reaction patterns, we conducted quantitative polymerase chain reaction (qPCR) analyses on selected brain regions of B6 and BTBR mice exposed to either a social stimulus (a novel same-sex mouse) or a chemogenetic activation of OXT^{PVN} neurons (OXT-PVN)(Fig. 5). We analyzed genes that are relevant to OXT neuronal activation via the PVN circuit, including *c-fos* (as a neural activity

marker), *OXT*, OXT receptors (*OXTR*), vasopressin (*AVP*), and vasopressin 1a receptors (*AVPR1a*) in the PVN and its projecting regions, MeA, BnST, and septum.

In both B6 and BTBR mice, an increase in *c-fos* mRNA expression was observed in all selected regions following a social encounter, and in the PVN by chemogenetic OXT^{PVN} activation. Social encounter induced *OXT* gene expression in the PVN of both strains and *OXTR* mRNA in the MeA and BnST of B6 mice, but not of BTBR mice. In addition, the social encounter increased *AVPR1a* gene expression in the septum of B6 and BTBR mice. Chemogenetic activation of OXT^{PVN} neurons downregulated *OXT* gene expressions in the PVN and *AVPR1a* expressions in the BnST of both strains. The chemogenetic OXT^{PVN} activation also upregulated *OXTR* expressions in the MeA of both strains, while in the BnST, changes in the *OXTR* mRNA expression (upregulation) were only observed in B6 mice but not in BTBR mice, which represents only strain difference in mRNA expression pattern following a chemogenetic activation examined in the present study.

Discussion

OXT circuit-dependent regulation of socio-emotional behavior

Hypothalamic neuronal network plays a predominant role in valence processing of socio-emotional behaviors [43–44]. OXT neurons in the PVN are responsive to dynamic control of approach/avoidance behaviors in social and non-social contexts with a circuit-dependent fashion. We provide strong evidence that the $OXT^{PVN}\rightarrow^{MeA}$ circuit activates social approach behavior, along with anxiogenic profile, while the $OXT^{PVN}\rightarrow^{BnST}$ circuit inhibits social approach, accompanied by anxiolytic response. Social encounter with an unfamiliar counterpart induces c-Fos across the rostral-to-caudal portions of the PVN and its projecting regions, including the BnST (only anterior portion) and MeA, in which the induction of OXT receptor genes was also evident. Chemogenetic stimulation of OXT^{PVN} neurons that concurrently activates both $OXT^{PVN}\rightarrow^{BnST}$ neurons and $OXT^{PVN}\rightarrow^{MeA}$ neurons upregulates the OXT receptor gene expression in both the BnST and MeA; however, suppresses social approach behavior. Therefore, $OXT^{PVN}\rightarrow^{BnST}$ signal that suppresses social approach is significantly effective than $OXT^{PVN}\rightarrow^{MeA}$ signal that generally facilitates social approach when both circuits are simultaneously activated. Social encounter per se induces approach behavior accompanied by the upregulation of OXT receptor gene expression and c-Fos in the MeA and anterior BnST; thus, the $OXT^{PVN}\rightarrow^{MeA}$ signal takes priority to control their behaviors over those $OXT^{PVN}\rightarrow^{BnST}$ signal in a prosocial context. A possible key determinant for OXT circuit balance would act by an inhibitory mediator in the downstream of OXT pathway in the BnST. The posterior BnST and MeA are anatomically characterized as a set of interneuronal nuclei, called as the extended amygdala [45]. It is likely that certain interneuronal connection relayed between the BnST and MeA acts to adjust output balance of neural signals from investigatory approach to non-social stimuli (i.e., $OXT^{PVN}\rightarrow^{BnST}$ signal) to craving approach to prosocial stimuli (i.e., $OXT^{PVN}\rightarrow^{MeA}$ signal).

Accordingly, the MeA–posterior BNST circuits projecting to the hypothalamus are responsible for innate social and predator-defense behaviors [46–47]. Further research is needed to elucidate whether molecular pathway of the OXT circuits maintains balancing of their output within the PVN interneuronal connections or across the inter-regional connections, such as the MeA-posterior BnST circuits.

Defect of OXT neural circuits accompanied by social deficits in an ASD mouse model

BTBR mice exhibit typical behavioral profile resembling the characteristics of human ASD, including impaired prosocial interaction and persistent, repetitive behaviors [25–26]. Although a target neuronal circuit responsible for controlling these social and non-social deficits exhibited by ASD animal models have been investigated for more than a decade, little is known about the circuit mechanism underlying these behavioral impairments. BTBR mice exhibit decreased densities of OXT neurons across the PVN sub-portions. Furthermore, the $OXT^{PVN \rightarrow BnST}$ circuit, which is massively expressed in B6 mice, appears to be defected in BTBR mice. These malformations of OXT circuit would be linked to blunted responses of neuronal activity patterns across the PVN and its projecting regions following a social encounter. While there is certain dissociation between protein level (e.g., c-Fos IHC) and mRNA level (e.g., *c-fos* qPCR) in response to a social stimulus exposure, the $OXT^{PVN \rightarrow BnST}$ circuit is documented to be defective but the $OXT^{PVN \rightarrow MeA}$ circuit is still intact in BTBR mice.

We recently reported a circuit dysfunction in BTBR mice that shows a compromised circuit in the posterior BnST to the lateral habenula, possibly via attenuating vasopressinergic signal/projection, which contributes to a lack of coordinative responses of social signaling by BTBR mice in a social context [29]. Our present data can extend it to an OXT circuit defect of BTBR mice for controlling prosocial behavior. BTBR mice exhibits agenesis of several brain structures, including the absence of corpus callosum, atrophic of hippocampus, and glial cells overexpression in the cingulate cortex [29, 48]. A MRI imaging analysis revealed that decreased cortical and thalamic grey matter volume along with a reduction of cortical thickness are documented in BTBR mice [49]. It is indicated that one of these morphological mutations occurs in developing brain network of BTBR mice, resulting in a subsided OXT signals and coordinative circuit function that are required to express appropriate approach/avoidance behavior in a social and non-social context.

Non OXT neurons in the PVN are involved in controlling non-social, defensive components

A pathological repetitive behavior is one of the core symptoms diagnosed as ASD [50]. An underlying mechanism for this exploited behavior would be distinguishable from those for social deficit, although it is still under debate [51–52]. In rodent models, excessive self-grooming and persistent digging/burying the cage bedding materials are considered to recapitulate pathological repetitive behavior states expressed in ASD patients [41]. BTBR mice have repeatedly confirmed these excessive behavioral profiles [25, 33, 53]. Interestingly, nursing with a different, non-ASD, strain can modify social deficits in BTBR mice,

but cannot improve their excessive self-grooming [54], suggesting a possibility that different behavioral domains relevant to ASD symptom may be regulated by distinct brain mechanisms. Our data clearly demonstrated that OXT neurons in the PVN are not involved in the responsible mechanism for controlling excessive behavioral profiles, but rather non-OXT neurons in the PVN can stimulate these behaviors including self-grooming and digging/burying cage bedding.

A growing number of pharmacological manipulations on excessive self-grooming behaviors of BTBR mice have fault to archive consistent effects, including the use of cholinergic, glutaminergic, or serotonergic agents [53, 55–57]. Highly complicated, sequential organization of grooming (and related defensive) behaviors raises a hypothesis that various neural circuits regulating discrete components of complex behaviors (e.g., motor, strategy, and sequencing) are involved. Non-OXT PVN neurons offer to facilitate grooming and related obsessive components in both B6 and BTBR mice. The PVN is a multitransmitter nucleus controlling various biological functions [35]. A major stress-related hormone, corticotropin-releasing hormone (CRH) produced in the PVN, are known to induce self-grooming [58–59]. Furthermore, virally induced selective manipulation of vasopressin neurons in the PVN can modify self-grooming in mouse models [60]. These suggest that stress-related, OXT-independent mechanism would be a key mediator for controlling compulsive and defensive components of behavior in the PVN.

Conclusions

The data demonstrate a circuit-dependent role for OXT signaling in the PVN neurons in controlling social and emotional behaviors and illustrate that the coordinative regulation of two discrete OXT circuits; the $OXT^{PVN \rightarrow BnST}$ and $OXT^{PVN \rightarrow MeA}$ circuits, underlies to control these behaviors. A functional defect of the $OXT^{PVN \rightarrow BnST}$ signal coincides with prosocial behavioral deficits in BTBR mouse model of autism. The study provides novel information about the coordinative role of OXT circuits and establish a foundation for further investigations that delineate the circuit mechanisms of OXT signaling impacting prosocial processes and social deficits relevant to ASD symptom [61].

Declarations

Acknowledgements

This study was supported by JSPS KAKENHI Grant Number JP19K24681 (HA) and JSPS KAKENHI Grant Number JP20K16232 (YH), and by NINDS grant R34NS121875 (AO). This research in terms of AAV production was supported by the program for Brain Mapping by Integrated Neurotechnologies for Disease Studies (Brain/MINDS) from Japan Agency for Medical Research and Development (AMED) under Grant Number JP21dm0207113 and JP21dm0207111.

Author contributions

AO and HA designed the research, HA performed the research, YH and HA analyzed the data, and AO and HA wrote the paper.

Competing interest

No authors have financial relationships with commercial interests, and the authors declare no competing interests.

References

1. Carstensen LL. Motivation for social contact across the life span: a theory of socioemotional selectivity. Nebr Symp Motiv. 1992;40:209–54.
2. Carter CS. Neuroendocrine perspectives on social attachment and love. Psychoneuroendocrinol. 1998;23:779–818.
3. Doulames VM, Vilcans M, Lee S, Shea TB. Social interaction attenuates the extent of secondary neuronal damage following closed head injury in mice. Front. Behav. Neurosci. 2015;9:275.
4. Heinrich LM, Gullone E. The clinical significance of loneliness: a literature review. Clin Psychol Rev. 2006;26:695–718.
5. Kennedy DP, Adolphs R. The social brain in psychiatric and neurological disorders. Trends Cogn Sci. 2012;16(11):559–72.
6. Arakawa H. Ethological approach to social isolation effects in behavioral studies of laboratory rodents. Behav Brain Res. 2018;341:98–108.
7. Hsiao YH, Chang CH, Gean PW. Impact of social relationship on Alzheimer's memory impairment: mechanistic studies. J Biomed Sci. 2018;25:3.
8. Gimpl G, Fahrenholz F. The oxytocin receptor system: structure, function, and regulation. Physiol Rev. 2001;81(2):629–83.
9. Carter CS. The oxytocin-vasopressin pathway in the context of love and fear. Front. Endocronol. 2017;8:356.
10. Arakawa H. Dynamic regulation of oxytocin neuronal circuits in the sequential processes of prosocial behavior in rodent models. Curr Res Neurobiol. 2021;2:100011.
11. Landgraf R, Neumann ID. Vasopressin and oxytocin release within the brain: a dynamic concept of multiple and variable modes of neuropeptide communication. Front Neuroendocrinol. 2004;25(2–4):150–76.
12. Jurek B, Neumann ID. The oxytocin receptor: from intracellular signaling to behavior. Physiol Rev. 2018;98:1805–908.
13. Liao P-Y, Chiu Y-M, Yu J-H, Chen S-K. Mapping central projection of oxytocin neurons in unmated mice using cre and alkaline phosphatase reporter. Front Neuroana. 2020;14: 559402.
14. Ferguson JN, Adag JM, Insel TR, Young LJ. Oxytocin in the medial amygdala is essential for social recognition in the mouse. J Neurosci. 2001;21:8278–85.
15. Arakawa H, Arakawa K, Deak T. Oxytocin and vasopressin in the medial amygdala differentially modulate approach and avoidance behavior toward illness-related social odor. Neurosci.

2010;171:1141–51.

16. Yao S, Bergan J, Lanjuin A, Dulac C. Oxytocin signaling in the medial amygdala is required for sex discrimination of social cues. eLife. 2017;31373.
17. Duque-Wilckens N, Torres LY, Yokoyama S, Minie VA, Tran AM, Petkova SP, Hao R, et al. Extrahypothalamic oxytocin neurons drive stress-induced social vigilance and avoidance. PNAS. 2020;117(42):26406–13.
18. Herman JP, Tasker JG. Paraventricular hypothalamic mechanisms of chronic stress adaptation. Front Endocrinol. 2016;7:137.
19. Lin X, Itoga CA, Taha S, Li MH, Chen R, Sami K, Berton F, Francesconi W, Xu X. c-Fos mapping of brain regions activated by multi-modal and electric foot shock stress. Neurobiol Stress. 2018;8:92–102.
20. Jacob S, Brune CW, Carter CS, Leventhal BL, Lord C, Cook Jr EH. Association of the oxytocin receptor gene (OXTR) in Caucasian children and adolescents with autism. Neurosci. Lett. 2007;417:6–9.
21. Meyer M, Jurek B, Alfonso-Prieto M, Ribeiro R, Milenkovic VM, Winter J, et al. Structure-function relationships of the disease-linked A218T oxytocin receptor variant. Mol Psychiatry 2022;27:907–17.
22. Bales KL, Solomon M, Jacob S, Crawley JN, Silverman JL, Larke RH, Sahagun E, Puhger KR, Pride MC, Mendoza SP. 2014. Long-term exposure to intranasal oxytocin in a mouse autism model. Transl Psychiatry 2014;4:e480.
23. Sikich L, et al. Intranasal oxytocin in children and adolescents with autism spectrum disorder. New Engl J Med. 2021;385:1462–73.
24. Ergaz Z, Weinstein-Fudim L, Ornoy A. Genetic and non-genetic animal models for autism spectrum disorders (ASD). Reprod Toxicol. 2016;64:116–40.
25. McFarlane HG, Kusek GK, Yang M, Phoenix JL, Bolivar VJ, Crawley JN. Autism-like behavioral phenotypes in, BTBR T + tf/J mice. Genes Brain Behav 2008;7:152–63.
26. Blanchard DC, Defensor EB, Meyza KZ, Pobbe RLH, Pearson BL, Bolivar VJ, Blanchard RJ. BTBR T + tf/J mice: autism-relevant behaviors and reduced fractone-associated heparan sulfate. Neurosci Biobehav Rev. 2012;36:285–96.
27. Tartaglione AM, Farioli Vecchioli S, Giorgi MC, Cutuli D, Calamandrei G. Altered responsiveness to pups in virgin female mice of the BTBR strain: insights from pattern of c-Fos expression in brain regions involved in maternal behavior. Behav Brain Res. 2021;410: 113365.
28. Meyza K, Nikolaev T, Kondrakiewicz K, Blanchard DC, Blanchard RJ, Knapska E. Neuronal correlates of asocial behavior in a BTBR T (+) Itpr3(tf)/ J mouse model of autism. Front Behav Neurosci. 2015;9:199.
29. Higuchi Y, Tachigori S, Arakawa H. Faded neural projection from the posterior bed nucleus of the stria terminalis to the lateral habenula contributes to social signaling deficit in male BTBR mice as a mouse model of autism. Psychoneuroendocrinol. 2023;149:106004.
30. Dölen G, Darvishzadeh A, Wui Huang K, Malenka RC. Social reward requires coordinated activity of nucleus accumbens oxytocin and serotonin. Nature. 2013;501(7466):179–84.

31. Eliava M, Melchior M, Knobloch-Bollmann HS, Wahis J, da Silva Gouveia M, Tang Y, et al. A new population of parvocellular oxytocin neurons controlling magnocellular neuron activity and inflammatory pain processing. Neuron. 89(6):1291–1304.
32. Walf AA, Frye CA. The use of the elevated plus maze as an assay of anxiety-related behavior in rodents. Nat Protocols. 2007;2:322–28.
33. Pobbe RLH, Pearson BL, Defensor EB, Bolivar VJ, Blanchard DC, Blanchard RJ. Expression of social behaviors of C57BL/6J versus BTBR inbred mouse strains in the visible burrow system. Behav Brain Res. 2010;214:443–9.
34. Langley EA, Krykbaeva M, Blusztajin JK, Mellott TJ. High maternal choline consumption during pregnancy and nursing alleviates deficits in social interaction and improves anxiety-like behaviors in the BTBR T + Itpr3tf/J mouse model of autism. Behav Brain Res. 2015;278: 210–20.
35. Herman JP, Tasker JG. Paraventricular hypothalamic mechanisms of chronic stress adaptation. Front Endocrinol. 7:137.
36. Kirouac GJ. The paraventricular neucleus of the thalamus as an integrating and repay node in the brain anxiety network. Front Behav Neurosci. 2021;15:627633.
37. Neumann ID, Slattery DA. Oxytocin in general anxiety and social fear: a translational approach. Biol Psychiatry. 2016;79:213–21.
38. Duque-Wilckens N, Steinman MQ, Busnelli M, Chini B, Yokoyama S. et al. Oxytocin receptors in the anteromedial bed nucleus of the stria terminalis promote stress-induced social avoidance in female california mice. Biol Psychiatry. 2018;83:203–13.
39. Defensor EB, Pearson BL, Pobbe RL, Bolivar VJ, Blanchard DC, Blanchard RJ. A novel social proximity test suggests patterns of social avoidance and gaze aversion-like behavior in BTBR T + tf/J mice. Behav Brain Res. 2011;217(2):302–8.
40. Feusner JD, Hembacher E, Phillips KA. The mouse who couldn't stop washing: pathologic grooming in animals and humans, CNS Spectr. 2009;14(9):503–13.
41. Kalueff AV, Stewart AM, Song C, Berridge KC, Graybiel AM, Fentress JC. Neurobiology of rodent self-grooming and its value for translational neuroscience, Nat Rev Neurosci. 2016;17(1):45–59.
42. Rosen JB, Asok A, Chakraborty T. The smell of fear: innate threat of 2,5-dihydro-2,4,5-trimethylthiazoline, a single molecule component of a predator odor. Front Neurosci. 2015;9:292.
43. Kunwar PS, Zelikowsky M, Remedios R, Cai H, Yilmaz M, Meister M, Anderson DJ. Venromedial hypothalamic neurons control a defensive emotion state. eLife. 2015;4:e06633.
44. Pessoa L. A network model of the emotional brain. Trends Cogn Sci. 2017;21(5):357–71.
45. Lebow MA, Chen A. Overshadowed by the amygdala: the bed nucleus of the stria terminalis emerges as key to psychiatric disorders. Mol. Psychiatry. 2016;21:450–63.
46. Friedman A, Homma D, Gibb LG, Amemori K, Rubin SJ, Hood AS, et al. A corticostriatal path targeting striosomes controls decision-making under conflict. Cell. 2015;161(6):1320–33.

47. Flanigan ME, Kash TL. Coordination of social behaviors by the bed nucleus of the stria terminalis. Eur J Neurosci. 2022;55(9–10):2404–20.
48. Stephenson DT, O'Neill SM, Narayan S, Tiwari A, Arnold E, Samaroo HD, et al. Histophathologic characterization of the BTBR mouse model of autistic-like behavior reveals selective changes in neurodevelopmental proteins and adult hippocampal neurogenesis. Mol Autism. 2011;2:7.
49. Dodero L, Damiano M, Galbusera A, Bifone A, Tsaftsaris SA, Scattoni ML. Neuroimaging evidence of major morpho-anatomical and functional abnormalities in the BTBR T + TFjJ mouse model of autism. PLOS One. 2013;8(10):e76655.
50. Boyd BA, McDonough SG, Bodfish JW. Evidence-based behavioral interventions for repetitive behaviors in autism, J Autism Dev Disord. 2012;42:1236–48.
51. Szatmari P, Georgiades S, Bryson S, Zwaigenbaum L, Roberts W, Mahoney W, et al. Investigating the structure of the restricted, repetitive behaviours and interests domain of autism. J Child Psychol Psychiatry. 2006;47:582–90.
52. Arakawa H. From multisensory assessment to functional interpretation of social behavioral phenotype in transgenic mouse models for autism spectrum disorders, Front Psychiatry 2020;11:592408.
53. Arakawa H. Implication of the social function of excessive self-grooming behavior in BTBR T + ltpr3tf/J mice as an idiopathic model of autism. Physiol Behav. 2021;237:113432.
54. Yang M, Perry K, Weber MD, Katz AM, Crawley JN. Social peers rescue autism-relevant sociability deficits in adolescent mice. Autism Res. 2011;4:17–27.
55. Athnaiel O, Job GA, Ocampo R, Teneqexhi P, Messer WS, Ragozzino ME. Effects of the partial M1 muscarinic cholinergic receptor agonist CDD-0102A on stereotyped motor behaviors and reversal learning in the BTBR mouse model of autism. Int J Neuropsychopharmacol. 2022;25(1):64–74.
56. Silverman JL, Tolu SS, Barkan CL, Crawley JN. Repetitive self-grooming behavior in the BTBR mouse model of autism is blocked by the mGluR5 antagonist MPEP. Neuropsychopharmacol. 2010;35:976–89.
57. Amodeo DA, Oliver B, Pahua A, Hitchcock K, Bykowski A, Tice D, et al. Serotonin 6 receptor blockade reduces repetitive behavior in the BTBR mouse model of autism spectrum disorder, Pharmacol Biochem Behav. 2021;200:173076.
58. Füzesi T, Daviu N, Wamsteeker Cusulin JI, Bonin RP, Bains JS. Hypothalamic CRH neurons orchestrate complex behaviours after stress. Nat Comm. 2016;7:11937.
59. Roseberry AG, Stuhrman K, Dunigan AI. Regulation of the mesocorticolimbic and mesostriatal dopamine systems by alpha-melanocyte stimulating hormone and agouti-related protein. Neurosci Biobehav Rev. 2015;56:15–25.
60. Islam MT, Maejima T, Matsui A, Mieda M. Paraventricular hypothalamic vasopressin neurons induce self-grooming in mice. Mol Brain. 2022;15:47.
61. Walsh JJ, Christoffel DJ, Makenka RC. Neural circuits regulating prosocial behaviors. Neuropsychopharmacol. 2023;48:79–89.

62. Pobbe RLH, Defensor EB, Pearson BL, Bolivar VJ, Blanchard DC, Blanchard RJ. General and social anxiety in the BTBR T + tf/J mouse strain. Behav. Brain Res. 2012;216:446–51.
63. Kirihara Y, Takechi M, Kurosaki K, Kobayashi Y, Kurosawa T. Anesthetic effects of a mixture of medetomidine, midazolam and butorphanol in two strains of mice. Exp Anim. 2013;62 (3):173–80.
64. Arakawa H. Analysis of social process in two inbred strains of male mice: a predominance of context-based investigation in BALB/c mice. Neurosci. 2018;369:124–38.

Figures

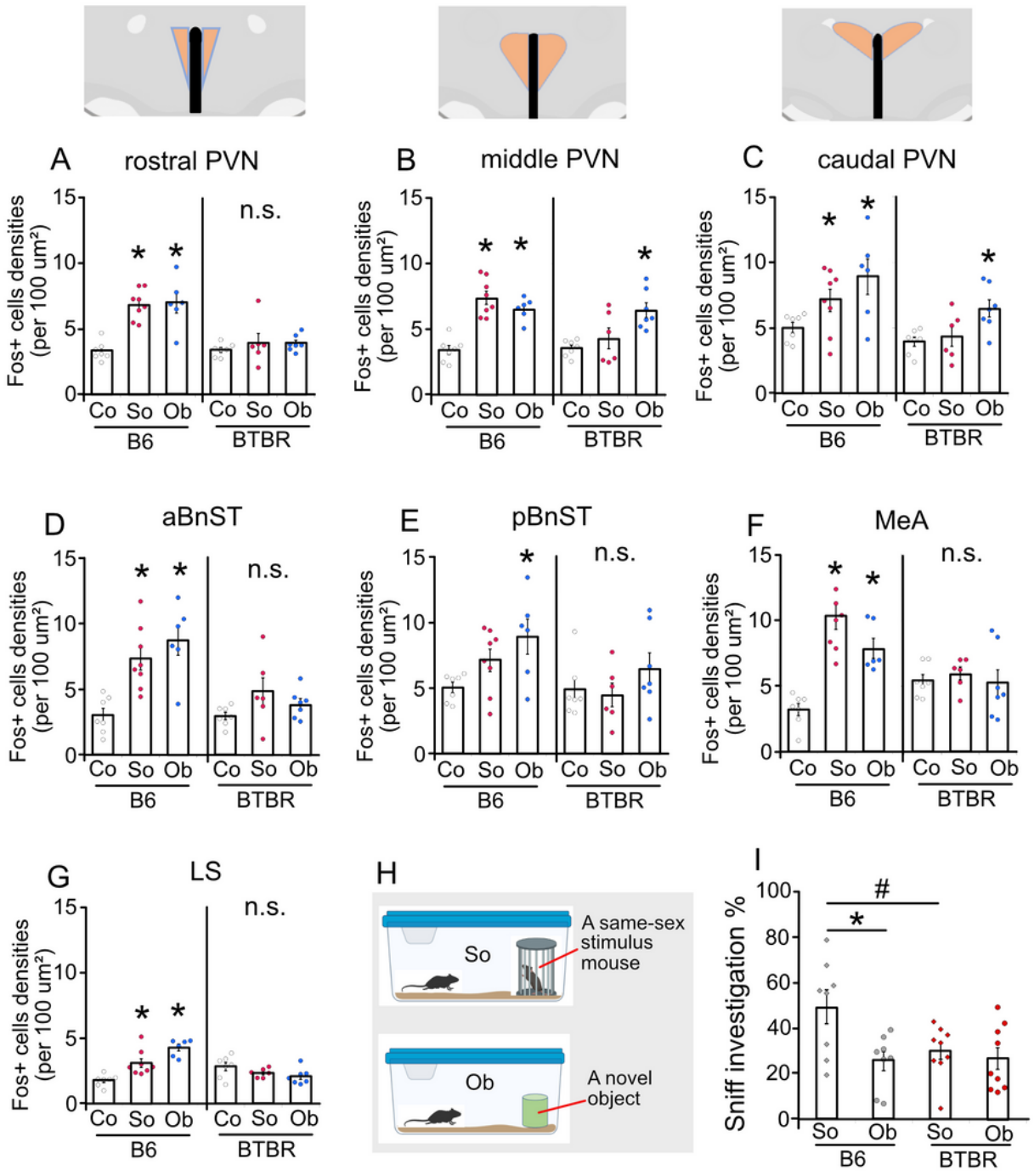


Figure 1

c-Fos induction is evident in B6 mice, in response to an exposure of an object (Ob) or social (So) stimuli, but blunted in BTBR in response to So exposure. Across the rostral (**A**, $F_{2,18} = 1.178$, $p < 0.0001$), middle (**B**, $F_{2,18} = 25.13$, $p < 0.0001$) to caudal (**C**, $F_{2,18} = 20.94$, $p = 0.0004$) PVN portions of B6 mice, induction of c-Fos is significantly increased both by object and social stimuli. The c-Fos induction is not revealed in the rostral PVN portion of BTBR mice ($F_{2,17} = 0.5842$, $p = 0.5683$), by either an object or social exposure,

while it was increased in the middle ($F_{2,17}$ = 7.687, p = 0.0042) and caudal PVN of BTBR mice ($F_{2,17}$ = 5.5772, p = 0.0137), following an object, but not social exposure. In B6 mice, c-Fos induction is shown in aBnST (**D**, $F_{2,18}$ = 11.732, p = 0.0005), MeA (**F**, $F_{2,18}$ = 21.11, p < 0.0001), and LS (**G**, $F_{2,18}$ = 18.787, p < 0.0001) following either object or social stimuli, and in pBnST (**E,** $F_{2,18}$ = 4.3158, p = 0.0294), only by an object exposure. However, these Fos inductions are not evident in BTBR mice in either aBnST ($F_{2,17}$ = 2.0808, p = 0.156), pBnST ($F_{2,17}$ = 1.2557, p = 0.31), MeA ($F_{2,17}$ = 0.2689, p = 0.767), or LS ($F_{2,17}$ = 2.4028, p = 0.1205), by either an object or social stimulus exposure. **H** Test conditions of stimulus exposure. **I** During the stimulus exposure, B6 and BTBR mice sniff/contact to a confronted object in similar level (p = 0.876), while BTBR mice exhibit lower sniff/contact than B6 mice to a confronted social stimulus (p = 0.0252) (2-way ANOVA, interaction of strain x stimuli, p = 0.056, main effect of strain, p = 0.0876, main effect of stimuli, p = 0.0127). * indicates difference between stimuli compared with homecage controls (Co), p < 0.05. # indicates difference between strain, p < 0.05. n.s., Not significant.

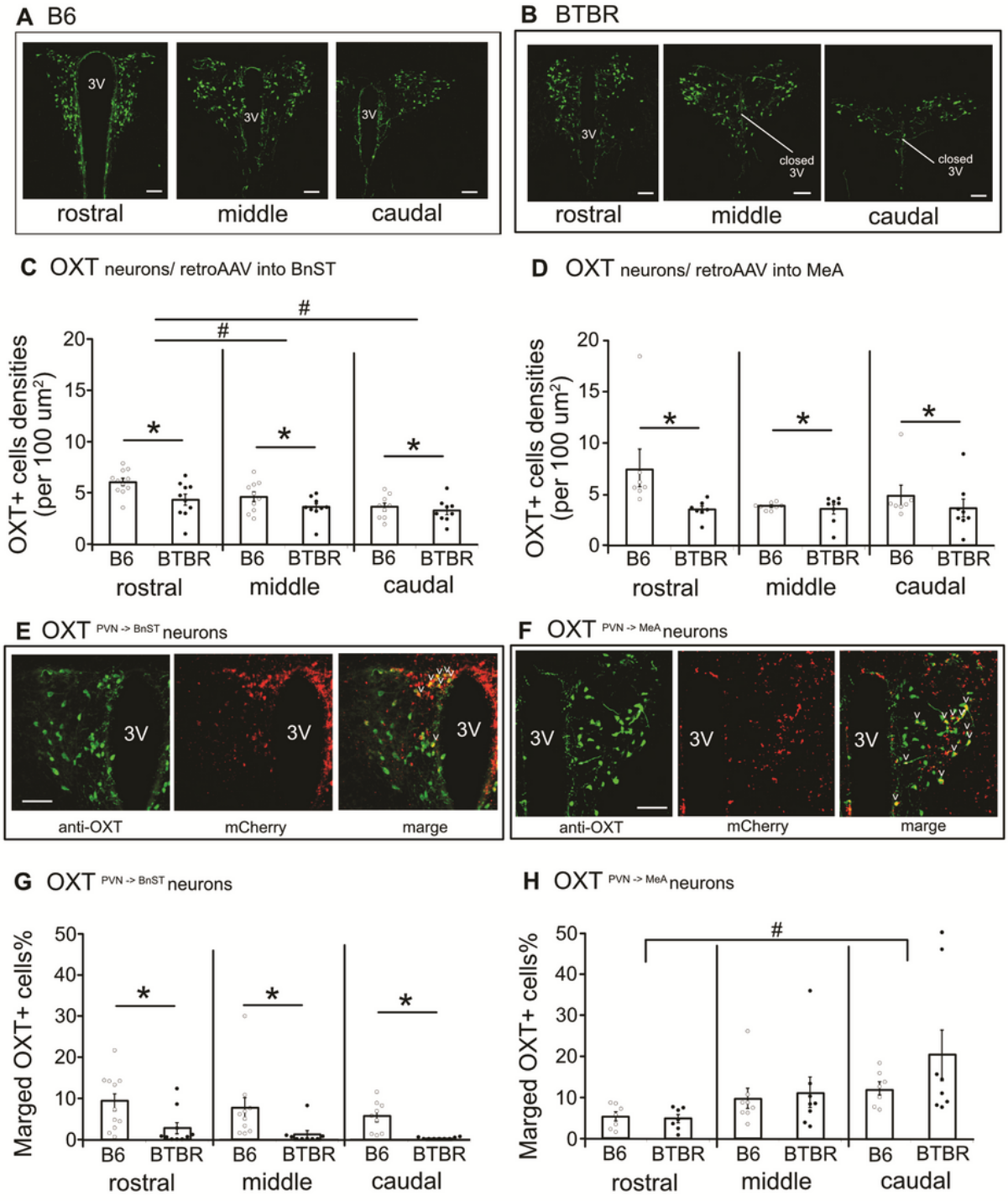


Figure 2

Densities of OXT+ cells are lower in BTBR mice than B6 mice across the rostral to caudal portions of the PVN. OXT$^{PVN->BnST}$ neurons are attenuated in BTBR, while those OXT$^{PVN->MeA}$ projecting neurons are consistently distributed both in BTBR and B6 mice. Representative immunostaining of anti-OXT antibody (green) across the rostral to caudal PVN of B6 (**A**) and BTBR (**B**) mice. **C** In both strains of mice received retroAAV (retroAAV-pOXT;mCherry) into BnST or **D** those received retroAAV into MeA, the densities of

OXT+ cells are higher in B6 than BTBR mice across the PVN portions (BnST, 2-way ANOVA, interaction of strain x PVN portion, $p = 0.298$, main effect of strain, $p = 0.0037$, main effect of PVN portion, $p = 0.00009$; MeA, 2-way ANOVA, interaction of strain x PVN portion, $p = 0.1182$, main effect of strain, $p = 0.0175$, main effect of PVN portion, $p = 0.1236$). **E,F** Representative pictures depict OXT+ cells (green), OXT promoter AAV infected cells (red), and those marged (yellow) neurons in B6 mice that were injected with AAV into the BnST ($OXT^{PVN->BnST}$ neurons; **E**) or those B6 mice received AAV injection into the MeA ($OXT^{PVN->MeA}$ neurons; **F**). **G** $OXT^{PVN->BnST}$ neurons are abundant in B6 mice, while those are faded in BTBR mice (2-way ANOVA, interaction of strain x PVN portion, $p = 0.9389$, main effect of strain $p = 0.0001$, main effect of PVN portion, $p = 0.2054$). **H** $OXT^{PVN->MeA}$ neurons are expressed in both B6 and BTBR mice and more dominant its distribution in the caudal PVN portion than rostral portion (2-way ANOVA, interaction of strain x PVN portion, p = 0.4421, main effect of strain, $p = 0.2942$, main effect of PVN portion, $p = 0.0098$). * indicates difference between strain, $p < 0.05$. # indicates difference between PVN portion, $p < 0.05$. n.s., Not significant. scale bar = 100 mm

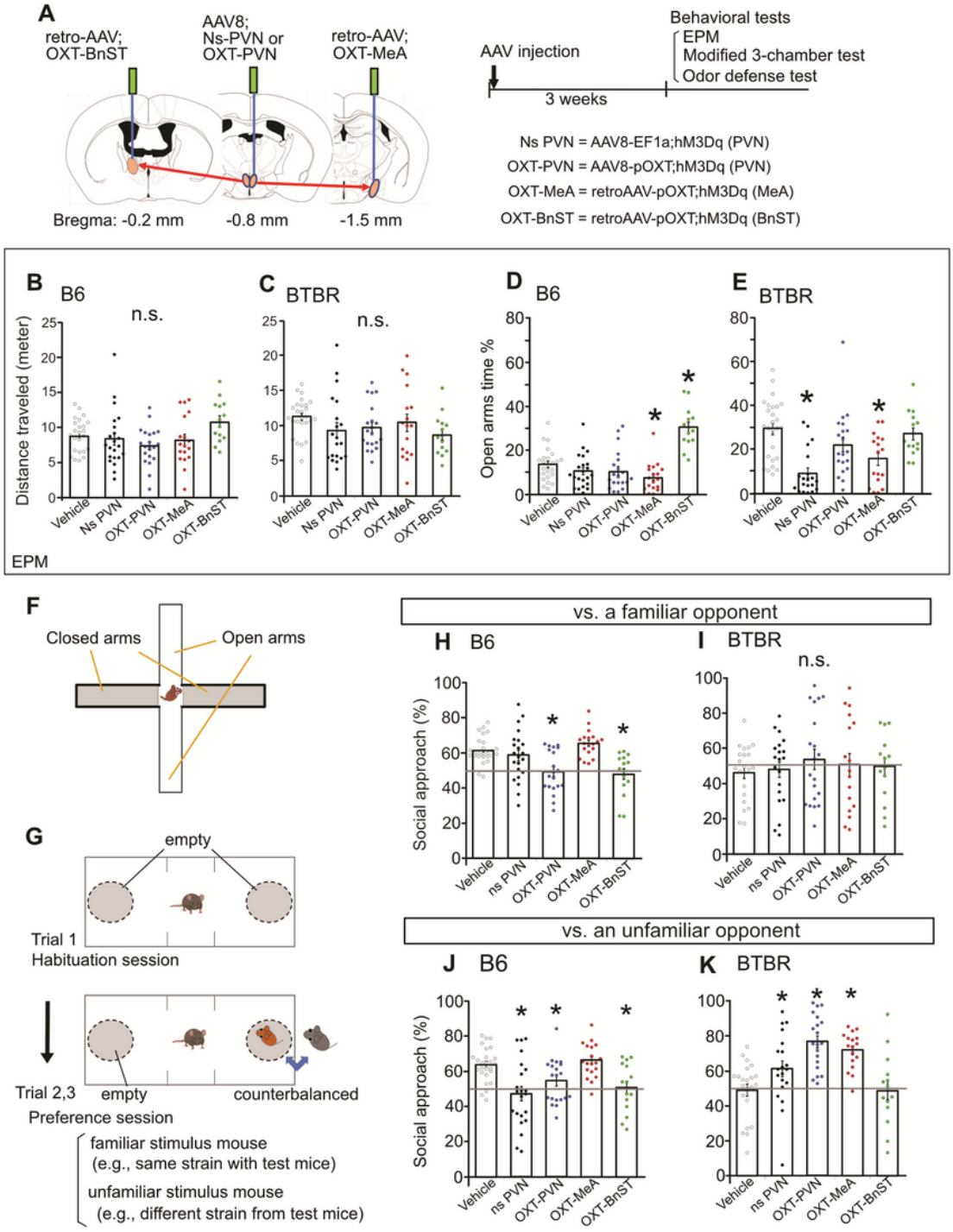


Figure 3

OXT$^{PVN->MeA}$ neurons differentially regulates anxiety-like behavior in the elevated plus maze (EPM) and social approach in the modified three chamber test from those OXT$^{PVN->BnST}$ neurons. A The viral strategy transfecting hM3Dq injected into the PVN, MeA, or BnST. **B,C** EPM. Chemogenetic activation of targeted neurons little impact on locomotor activity in B6 (2-way ANOVA, interaction of DREADD x sex, $p = 0.4989$, main effect of DREADD $p = 0.0721$, main effect of sex, $p = 0.5769$) or BTBR mice (2-way ANOVA,

interaction of DREADD x sex, p = 0.3128, main effect of DREADD, p = 0.4303, main effect of sex, p = 0.7447). **D** EPM. In B6 mice, activation of $OXT^{PVN->MeA}$ neurons decrease open-arm time % (p = 0.0485), while activation of those $OXT^{PVN->BnST}$ increase open-arm time % (p < 0.0001)(2-way ANOVA, interaction of DREADD x sex, p = 0.1853, main effect of DREADD p < 0.0001, main effect of sex, p = 0.164). **E** EPM. In BTBR mice, DREADD activation of non-specific PVN neurons (p < 0.0001) and those of $OXT^{PVN->MeA}$ neurons (p = 0.0019) decrease the open-arm time % (2-way ANOVA, interaction of DREADD x sex, p = 0.1728, main effect of DREADD, p < 0.0001, main effect of sex, p = 0.9219). **F** The elevated plus maze (EPM). **G** Procedure of the modified three-chamber test. **H** In B6 mice, chemogenetic activation of OXT^{PVN} neurons (p = 0.0007) and those of $OXT^{PVN->BnST}$ neurons (p = 0.0007) suppresses approach behavior towards a familiar stimulus mouse (2-way ANOVA, interaction of DREADD x sex, p = 0.8039, main effect of DREADD, p < 0.0001, main effect of sex, p = 0.9429). **I** In BTBR mice, any DREADD manipulation little affect approach behavior towards a familiar mouse (2-way ANOVA, interaction of DREADD x sex, p = 0.5664, main effect of DREADD p = 0.8688, main effect of sex, p = 0.862). **J** When confronted with an unfamiliar mouse, chemogenetic activation of non-specific PVN neurons (p = 0.0003), those of OXT^{PVN} neurons (p = 0.0369), and $OXT^{PVN->BnST}$ (p = 0.0095) induce a decreased social approach in B6 mice (2-way ANOVA, interaction of DREADD x sex, p = 0.9047, main effect of DREADD p < 0.0001, main effect of sex, p = 0.2178). **K** In BTBR mice, DREADD activation of non-specific PVN neurons (p = 0.0377), those of OXT^{PVN} neurons (p < 0.0001), or those of OXT $^{PVN->MeA}$ neurons (p = 0.0002) increased social approach (2-way ANOVA, interaction of DREADD x sex, p = 0.5473, main effect of DREADD, p < 0.0001, main effect of sex, p = 0.2483). * difference between DREADD compared with vehicle controls, p < 0.05. # difference between strain, p < 0.05. + difference between sex, p < 0.05. n.s., Not significant.

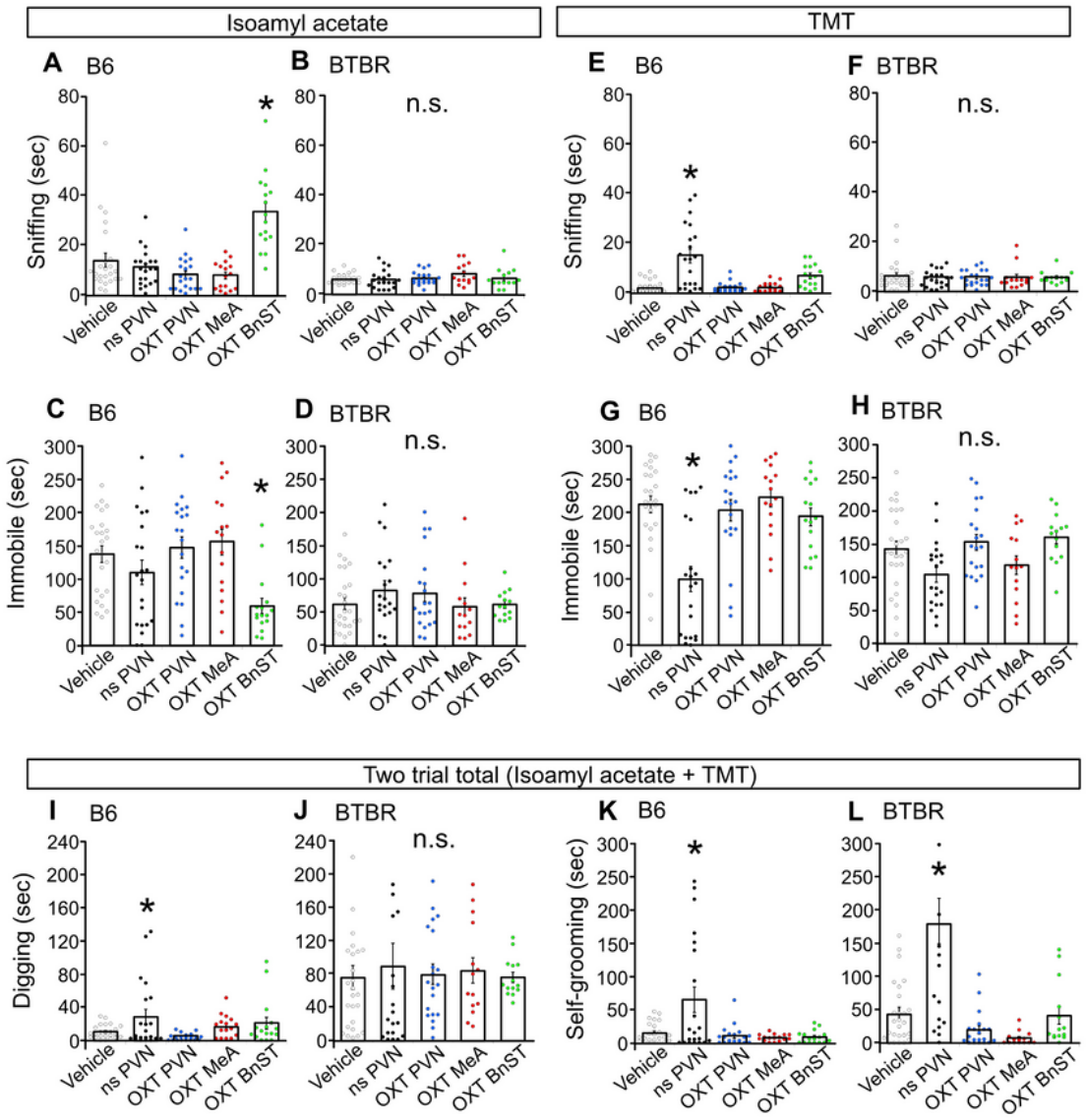


Figure 4

Non-OXT^{PVN} neurons are sufficient to mediate non-social, defensive behavior in both B6 and BTBR mice. **A,C** When exposed to a novel neutral odor (isoamyl acetate), chemogenetic activation of OXT$^{PVN->BnST}$ neurons increases sniffing ($p < 0.0001$)/decreases immobile ($p = 0.003$) in B6 mice (Sniffing: 2-way ANOVA, interaction of DREADD x sex, $p = 0.6609$, main effect of DREADD, $p < 0.0001$, main effect of sex, $p = 0.1331$, Immobile: 2-way ANOVA, interaction of DREADD x sex, $p = 0.6497$, main effect of DREADD, p

= 0.0011, main effect of sex, p = 0.0169). **B,D** There is no impact of DREADD on sniff/immobile towards exposure of a neutral odor in BTBR mice (Sniffing: 2-way ANOVA, interaction of DREADD x sex, p = 0.0411, main effect of DREADD, p = 0.1114, main effect of sex, p = 0.0018, Immobile: 2-way ANOVA, interaction of DREADD x sex, p = 0.8235, main effect of DREADD, p = 0.3805, main effect of sex, p = 0.547). **E,G** When confronted with a predatory odor (TMT), DREADD activation of non-specific PVN neurons increases sniffing (p < 0.0001) and decreases immobile (p < 0.0001) in B6 mice (Sniffing: 2-way ANOVA, interaction of DREADD x sex, p = 0.007, main effect of DREADD, p < 0.0001, main effect of sex, p = 0.0139, Immobile: 2-way ANOVA, interaction of strain x sex, p = 0.3804, main effect of DREADD, p < 0.0001, main effect of sex, p = 0.2179). **F,H** There is no effects of DREADD manipulation on sniff/immobile towards a predatory odor in BTBR mice (Sniffing: 2-way ANOVA, interaction of DREADD x sex, p = 0.8902, main effect of DREADD, p = 0.9555, main effect of sex, p = 0.2298, Immobile: 2-way ANOVA, interaction of DREADD x sex, p = 0.675, main effect of DREADD, p = 0.0273, main effect of sex, p = 0.7122). **I,J** Chemogenetic activation of non-specific PVN neurons increases digging in B6 (p = 0.032) but not in BTBR (B6: 2-way ANOVA, interaction of DREADD x sex, p = 0.8463, main effect of DREADD p = 0.0209, main effect of sex, p = 0.6105, BTBR: 2-way ANOVA, interaction of DREADD x sex, p = 0.5693, main effect of DREADD, p = 0.9812, main effect of sex, p = 0.9569). **K,L** Chemogenetic activation of non-specific PVN neurons increases self-grooming in both B6 and BTBR mice (ps < 0.0001) (B6: 2-way ANOVA, interaction of DREADD x sex, p < 0.0001, main effect of DREADD, p < 0.0001, main effect of sex, p < 0.0001, BTBR: 2-way ANOVA, interaction of DREADD x sex, p < 0.0001, main effect of DREADD, p < 0.0001, main effect of sex, p = 0.001). * difference between DREADD compared with vehicle controls, p < 0.05. n.s., Not significant.

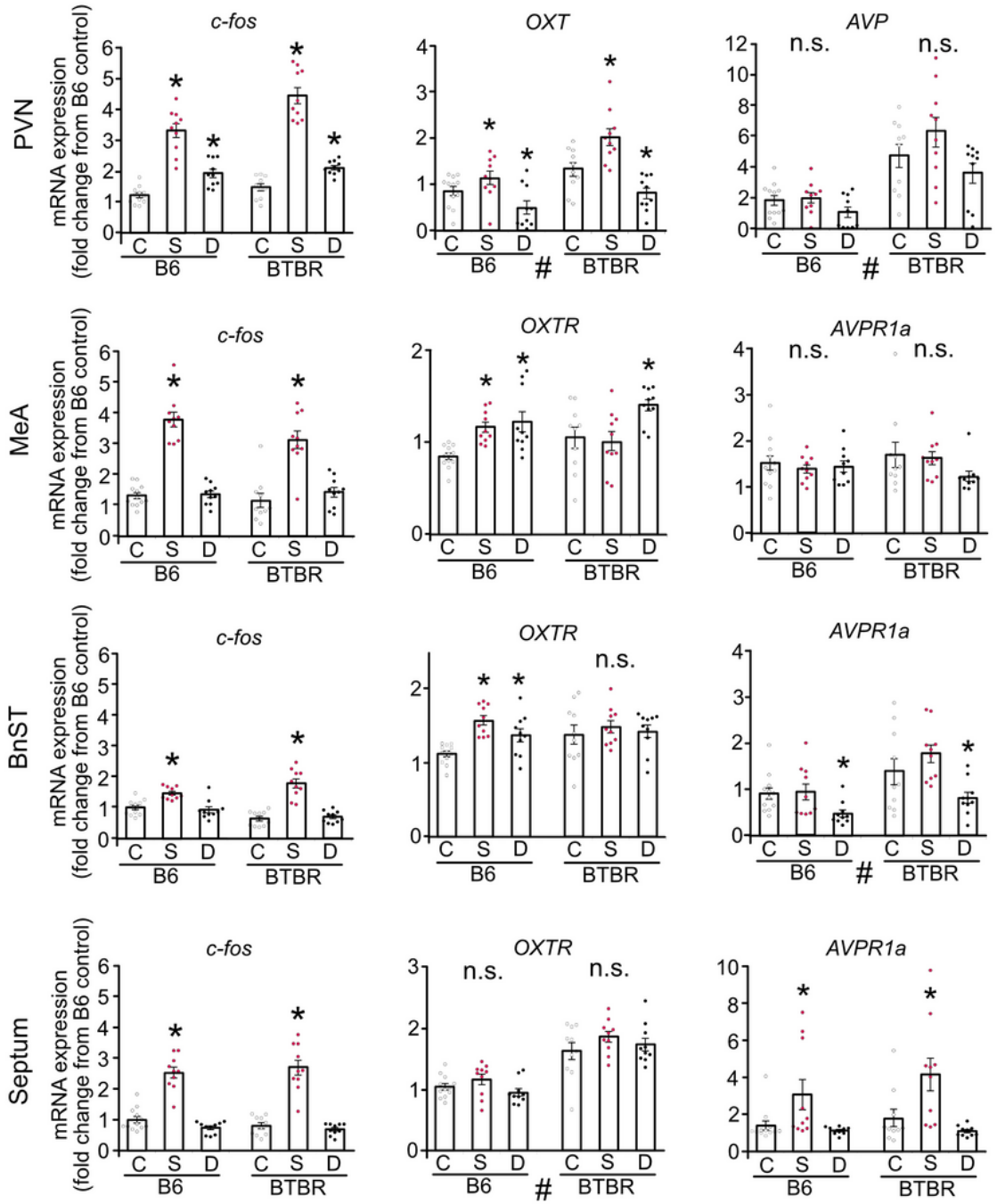


Figure 5

The mRNA expression of *c-fos*, *OXT*, and its homolog receptors (*OXTR* and *AVPR1a*) in the PVN and its projecting regions induced by social encounter (S) or chemogenetic activation of OXT^{PVN} neurons (D) in B6 and BTBR mice. In the PVN, *c-fos* expression is induced by both S and D in B6 and BTBR mice (2-way ANOVA, interaction of Strain x condition, $p = 0.0075$, main effect of strain, $p = 0.0002$, main effect of condition, $p < 0.0001$). *OXT* mRNA increases with S ($p < 0.0001$) and decreases with D ($p = 0.0204$) in

both B6 and BTBR mice (2-way ANOVA, interaction of strain x condition, $p = 0.6724$, main effect of strain, $p < 0.0001$, main effect of condition, $p = 0.0003$). *AVP* induction is more in BTBR mice than B6 mice (2-way ANOVA, interaction of strain x condition, $p = 0.3261$, main effect of strain, $p < 0.0001$, main effect of condition, $p = 0.0161$). In the MeA, *c-fos* expression is abundant by S ($p < 0.0001$) but not by D ($p = 0.4605$) (2-way ANOVA, interaction of strain x condition, $p = 0.175$, main effect of strain, $p = 0.1234$, main effect of condition, $p < 0.0001$). The *OXTR* mRNA increases with S ($p = 0.0048$) and D ($p = 0.002$), in B6 mice, while it increases with D ($p = 0.0223$), but not with S ($p = 0.7965$) in BTBR mice (2-way ANOVA, interaction of strain x condition, $p = 0.0727$, main effect of strain, $p = 0.258$, main effect of condition, $p = 0.0002$). *AVPR1a* mRNA is not altered by S or D in either B6 or BTBR mice (2-way ANOVA, interaction of strain x condition, ns $p = 0.3335$, main effect of strain, ns $p = 0.6085$, main effect of condition, ns $p = 0.2424$). In the BnST, *c-fos* mRNA increases with S ($p = 0.0003$) but not with D ($p = 0.4869$) in B6 and BTBR mice (2-way ANOVA, interaction of strain x condition, $p = 0.0008$, main effect of strain, $p = 0.3542$, main effect of condition, $p < 0.0001$). *OXTR* mRNA increases with S ($p = 0.0001$) or D ($p = 0.0138$) in B6 mice, while it is not altered by either S or D in BTBR mice (2-way ANOVA, interaction of strain x condition, $p = 0.0211$, main effect of strain, $p = 0.1229$, main effect of condition, $p = 0.0096$). *AVPR1a* mRNA decreases with D ($p = 0.0226$) in both B6 and BTBR mice (2-way ANOVA, interaction of strain x condition, $p = 0.3593$, main effect of strain, $p = 0.0002$, main effect of condition, $p = 0.0005$). In the septum, *c-fos* mRNA increases with S ($p < 0.0001$) but not with D ($p = 0.1526$) in B6 and BTBR mice (2-way ANOVA, interaction of strain x condition, $p = 0.4392$, main effect of strain, $p = 0.9381$, main effect of condition, $p < 0.0001$). *OXTR* mRNA induction is higher in BTBR mice than B6 mice (2-way ANOVA, interaction of strain x condition, $p = 0.5441$, main effect of strain, $p < 0.0001$, main effect of condition, $p = 0.1021$). *AVPR1a* mRNA increases with S ($p = 0.0006$) in both B6 and BTBR mice (2-way ANOVA, interaction of strain x condition, $p = 0.6726$, main effect of strain, $p = 0.2618$, main effect of condition, $p = 0.0007$). * difference between conditions compared with Controls, $p < 0.05$. n.s., Not significant.

Supplementary Files

This is a list of supplementary files associated with this preprint. Click to download.

- Supplementcombinedv5.pdf